Room-temperature ferromagnetism in Li-doped *p*-type luminescent ZnO nanorods

Santa Chawla,* K. Jayanthi, and R. K. Kotnala
National Physical Laboratory, Dr. K. S. Krishnan Road, New Delhi-110012, India
(Received 18 April 2008; revised manuscript received 16 January 2009; published 25 March 2009)

We have observed ferromagnetism in Li-doped ZnO nanorods with Curie temperature up to 554 K. Li forms shallow acceptor states in substitutional zinc sites giving rise to *p*-type conductivity. An explicit correlation emerges between increase in hole concentration with decrease in magnetization and Curie temperature in ZnO:Li. Occurrence of ferromagnetism at room temperature has been established with observed magnetic domain formation in ZnO:Li pellets in magnetic force microscopy and prominent ferromagnetic resonance signal in electron paramagnetic resonance spectrum. Magnetic ZnO:Li nanorods are luminescent, showing strong near UV emission. Substitutional Li atoms can induce local moments on neighboring oxygen atoms, which when considered in a correlated model for oxygen orbitals with random potentials introduced by dopant atom could explain the observed ferromagnetism and high Curie temperature in ZnO:Li nanorods.

DOI: 10.1103/PhysRevB.79.125204 PACS number(s): 75.50.Pp, 72.20.−i, 78.55.−m, 78.67.Bf

I. INTRODUCTION

Dilute ferromagnetic semiconductors (DMSs) with Curie temperature at or above room temperature form an exceptional class of materials with immense potential for spintronic and magneto-optic devices. Achieving magnetic ordering at ambient temperature for a versatile and technologically important semiconductor such as ZnO is very meaningful. Dilute ferromagnetism in oxide semiconductors generally has been reported with 3*d* dopants in ZnO particularly with Mn, Co, Ni, Fe, Cu, and V dopings.[1–3] Unexpected magnetization without transition metal has been reported in dielectric oxides such as HfO_2, ZrO_2,[4] and nonmagnetic oxides, e.g., ZnO,[5] hexaborides,[6] carbon-doped ZnO,[7] and in irradiated graphite.[8] The theory of Dietl *et al.*[9] suggests that carrier-induced ferromagnetism in Mn-doped *p*-type material may be observed at higher temperature. Occurrence of ferromagnetism that also at room temperature in alkali-atom-doped ZnO has not been reported before, and we report here the ferromagnetic ordering observed in *p*-type ZnO:Li nanoparticles. Such dilute ferromagnetism in a nonmagnetic oxide like ZnO solely induced by very low concentration of monovalent alkali atom has no precedence, and understanding the phenomenon poses a theoretical challenge.

In a semiconductor magnetic ordering, electrical and optical properties may be intricately interlinked. This has the potential to harness magnetically controlled semiconducting light emitters. In a quest to find ferromagnetism in *p*-type ZnO without transition metal, as is preferable for spintronic applications,[10] doping of monovalent alkali atom Li with single unpaired spin in ZnO was undertaken. A combined study of electrical, magnetic, as well as structural and photoluminescence (PL) properties of Li-doped ZnO was carried out to explore ferromagnetism and to understand the physics. Undoped ZnO is usually *n* type due to interstitial Zn and oxygen vacancy, and better *n*-type conduction has been obtained in Al-doped ZnO.[1] However, realization of *p*-type ZnO has proven to be difficult due to formation of deep acceptor levels, self-compensating effect, and low solubility of acceptor dopants. Hence, *p*-type conduction in ZnO requires incorporation of shallow acceptor levels which may be possible by substituting group I element Li in Zn site (Li_{Zn}) that creates one hole per alkali atom in the neighboring oxygen atom. Shallow Li acceptor level is reported to be formed at temperature between 450–600 °C with binding energy of 300 meV and gives rise to PL emission at 3.05 eV,[11–13] with PL output peaking at 500–550 °C synthesis temperature. The shallow acceptor center is no longer introduced at temperatures above 700 °C. At lower temperatures of growth, introduction of redundant Li atoms as interstitial (Li_i) and Li_i-Li_{Zn} complex inhibits the *p*-type conductivity.[11] Deep acceptor center has also been reported in ZnO forming at temperature above 750 °C and producing broad Gaussian luminescence band at 2.05 eV.[12] Such deep acceptor levels inhibit *p*-type conductivity.

II. EXPERIMENTS

Nanocrystalline powder of ZnO doped with Li (2–15 at. %) was synthesized by solid-state reaction method. A homogeneous solution of high-purity precursor materials, Zn $(CH_3COO)_2.2H_2O$ (1 M) and LiOH (0.02–0.15 M), in deionized water was prepared. The solution was oven dried. Dried precursor material was ground in agate mortar and mixed thoroughly, packed in a quartz boat and fired at 500 °C in air. Synthesis of ZnO:Li was repeated for different Li concentrations with excellent reproducibility. The amount of trace magnetic impurities in the precursor materials was in ppm level. The same precursor, Zn $(CH_3COO)_2.2H_2O$ (1 M), was used to synthesize undoped ZnO. Any possibility of magnetic contamination through accidental or trace impurities has been meticulously avoided during sample preparation. High-purity quartz boat without any metallic contamination was used for firing the sample in the furnace. The body color of synthesized ZnO: Li was grayish white powder for all Li concentrations.

Crystallographic phase identification was done by x-ray diffraction (XRD) using Brucker-AXS D8 Advance Diffractometer. The crystallite shape and morphology of the ZnO:Li nanocrystals were studied under transmission electron microscope (TEM) (make: JEM; model: JEOL 200 Cx). Energy dispersive spectroscopy (EDS) was carried out to see the

effect of doping as well as presence of any magnetic impurity. No trace magnetic impurity was detected in EDS measurements. Nature of electrical conduction and carrier density was measured by Hall effect on pellets made from the ZnO:Li nanocrystalline powder. Pellets were made by subjecting the powder to a pressure of 10 ton. Ohmic contacts were made on the pellets by silver paste. The contacts were cured at 350 °C, and thereafter the electrodes were soldered on silvered surface. Pellets were subsequently sintered at 500 °C for 30 min. Measurement of Hall effect was carried out in Van der Pauw configuration with a constant current of 100 μA using high-resolution instruments, with an accuracy of $\pm 1.5\%$. Hall measurements were repeated for different magnetic fields and different applied voltages on the same sample. The results showed no appreciable change in measured hole concentration. A Varian E-112 spectrometer at microwave frequency of 9.11 GHz was used for electron paramagnetic resonance (EPR) measurements at ambient temperature. Magnetization (M-H) of the ZnO:Li powder samples was measured at room temperature using Lakeshore 7304 vibrating sample magnetometer (VSM) using a sample holder of high-purity perspex free from any metallic impurity. Extreme care was taken to clean the holder ultrasonically to remove any magnetic material traces. The same holder was used exclusively for measurement of ZnO samples to avoid any magnetic contamination. Same measurement procedure was repeated for empty sample holder, and magnetization data of the holder were subtracted from the measured magnetic signal of the sample. VSM has magnetization sensitivity on the order of 10^{-6} emu. Variation in magnetization with increase in temperature was recorded using VSM for Curie temperature determination. The results of magnetic measurements were reproducible ($\pm 5\%$) for all the samples. Repeated synthesis of ZnO:Li samples with different Li concentrations in different batches under same experimental conditions was carried out. Magnetic measurements done on different batches of ZnO:Li samples showed consistent and reproducible results. Atomic force microscopy (AFM) and magnetic force microscopy (MFM) were done with a high-resolution scanning probe microscope (SPM) attached with a magnetic probe (SPM multimode V, Veeco Instruments Inc., USA). Photoluminescence (PL) spectra and time-resolved decay of luminescence were recorded using a Xe-lamp source and Edinburgh Instruments combined FLSP920 steady state and lifetime spectrometer.

III. RESULTS AND DISCUSSION

Undoped ZnO and Li-doped ZnO samples crystallized in hexagonal wurtzite structure as is evident from x-ray diffraction pattern shown in Fig. 1. Lattice parameters a and c increase in the third place of decimal ($<0.1\%$) with incorporation of and variation in Li concentration. This indicates uniform doping of Li atoms in ZnO lattice. Such increase in a and c parameters with Li doping has also been reported for ZnO:Li films.[14] Zn-O bond length was calculated[14] to be 1.9679 Å for undoped ZnO and 1.9695 Å for 2 at. % Li, returning to undoped value for 10 at. % Li doping. Average crystallite size calculated from Scherrer formula ranges from

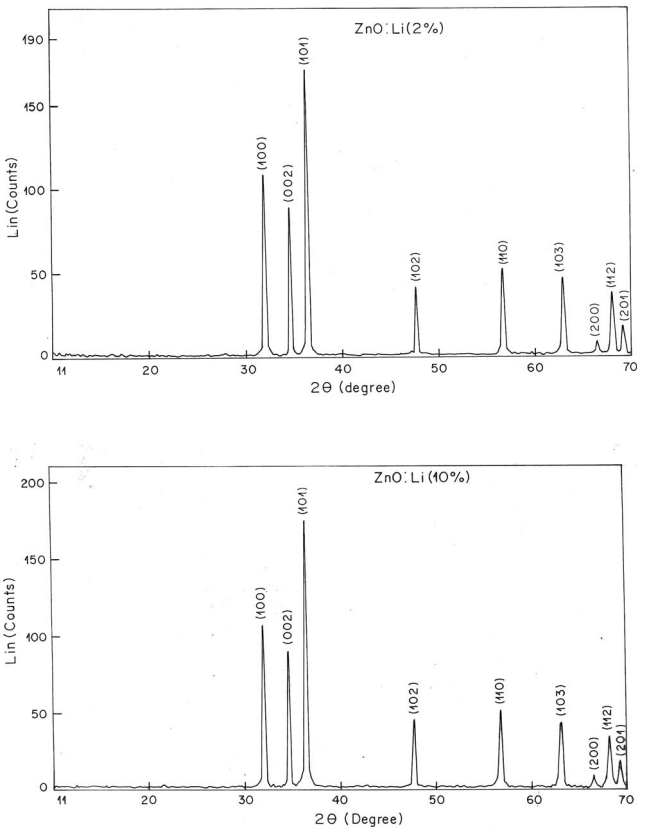

FIG. 1. XRD profile of ZnO:Li powder with 2 and 10% Li concentration showing monophasic hexagonal wurtzite structure.

52–72 nm. Scanning electron microscopy of the synthesized ZnO:Li powder showed elongated rod-type morphology of nanometer dimensions whereas 2% Li-doped ZnO exhibits best nanorod formation. *In situ* EDS measurement was done and no trace magnetic impurity was detected. TEM image (Fig. 2) showed well-formed single-crystal transparent nanorods of ZnO:Li (2 at. %). The length of the nanorods varied from 96 to 622 nm, and the diameter varied form 27 to 124 nm.

Hall-effect measurement carried out in Van der Pauw configuration exhibited n-type conductivity for undoped ZnO, whereas Li- (2–15 at. %) doped ZnO pellets showed p-type conductivity. Some shallow donor levels in undoped ZnO may give rise to n-type conduction. For ZnO:Li samples, hole concentration and resistivity vary with Li concentration

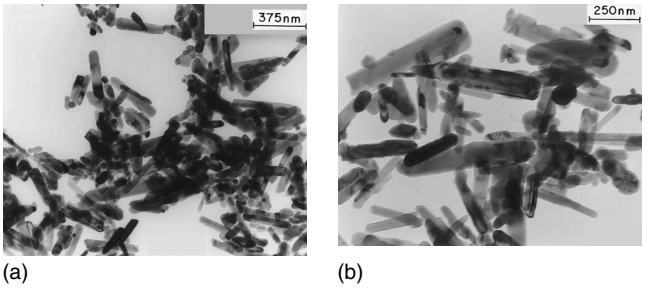

FIG. 2. TEM images of ZnO:Li (2 at. %) at two different magnifications showing well-developed transparent nanorods.

TABLE I. Variation of hole concentration and Curie temperature with Li concentration.

Li % (nominal)	Hole concentration (cm^{-3})	Resistivity k Ω cm	T_C (K)
2	1.6×10^{16}	107.5	554
5	8.4×10^{17}	95.0	394
10	2.5×10^{18}	76.4	344
15	1.3×10^{19}	43.7	diamagnetic

as shown in Table I. The results show a clear trend of hole concentration increase and resistivity decrease with increase in Li concentration. Results are in conformity with results reported for ZnO:Li thin film deposited at 500 °C giving rise to *p*-type conductivity with hole concentration on the order of 10^{16} cm^{-3}.[11,15] The results clearly indicate that Li atoms substitute zinc in zinc site to form shallow acceptor levels and that hole doping takes place in ZnO lattice. The increase in Madelung energy has been thought to facilitate localization of such acceptor states.[11]

Magnetization measurements carried out at room temperature for ZnO:Li nanocrystalline powder samples (as synthesized) with different nominal Li concentrations show typical ferromagnetic hysteresis loop for certain Li concentrations, as shown in Fig. 3. Undoped ZnO synthesized in exactly identical experimental conditions exhibits diamagnetism. Maximum magnetization observed for 2, 5, and 10 at. % Li are 55.71, 58.95, and 5.09 memu/g, respectively. A typical ferromagnetic narrow hysteresis loop was observed for ZnO:Li (2 at. %) sample with coercivity

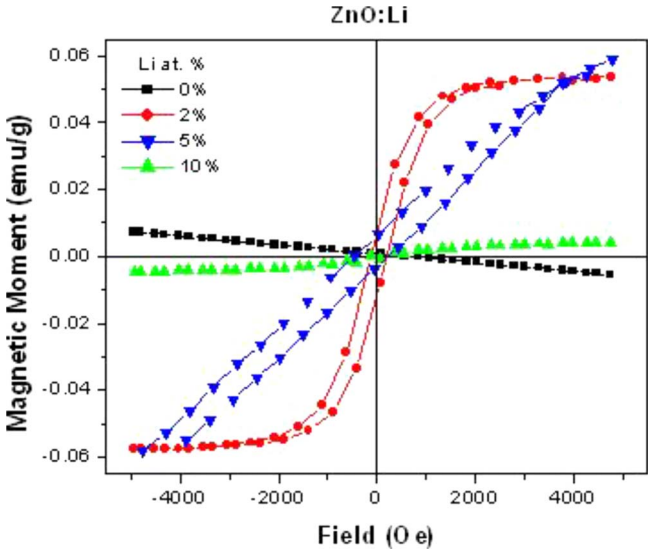

FIG. 3. (Color online) Observed magnetic moment with variation in magnetic field for ZnO:Li nanocrystalline powder at room temperature. ZnO:Li (2 at. %) exhibits typical ferromagnetic hysteresis loop. For 5% Li-doped samples, the *M-H* curve indicates super paramagnetic behavior. A decrease in magnetization was observed with further increase in Li concentration. Diamagnetic characteristic was shown by undoped ZnO prepared under similar conditions.

166.97 Oe and retentivity 9.62 memu/g with Curie temperature as high as 554 K. Li- (5 at. %) doped ZnO exhibited superparamagnetic behavior. Such superparamagnetic behavior has also been reported for ZnO:Ni thin films above 30 K.[16] Ferromagnetic behavior decreases with further increase in Li concentration in ZnO lattice. VSM has magnetization measurement sensitivity on the order of 10^{-6} emu, while our experimental results show magnetization on the order of 10^{-3} emu. Temperature-dependent magnetization study showed decrease in Curie temperature with increase in Li concentration in ZnO:Li as shown in Table I. Magnetic measurements were reproducible for all the ZnO:Li samples synthesized repeatedly in different batches under identical experimental conditions. Magnetization measurements were also carried out on the pellets used for Hall-effect measurement, and similar results were obtained as powder samples. In order to exclude any origin other than intrinsic to the observed magnetic behavior of ZnO:Li samples, sample synthesis, handling process, and measurements were done with utmost care. Since extreme precautions were taken during different steps involved in experimental process to avoid any magnetic contamination, only probable suspect could be trace magnetic impurities present in the precursor materials. Iron (Fe) was the only trace magnetic impurity present in the main precursor material $Zn(CH_3COO)_2.2H_2O$ (99.5%) in proportion of 0.0005% and also in the dopant precursor LiOH (0.005%). Since the same zinc acetate was used for preparation of undoped ZnO and ZnO:Li samples, the contribution of trace iron present in zinc acetate in producing ferromagnetism can be ruled out immediately as undoped ZnO synthesized under same conditions show pure diamagnetism. If trace iron in LiOH could be the cause for ferromagnetism then magnetization would have increased with increase in Li concentration. But experimental results clearly showed that magnetization was maximum for 2 at. % Li-doped ZnO where trace iron (Fe) would be only 0.0001%, and as Li concentration increased, magnetization decreased though the amount of trace Fe would have increased proportionately. As the results of all magnetic measurement conclusively show that ferromagnetism decreases with increase in Li concentration, the role of trace impurities in producing ferromagnetism in ZnO:Li can be ruled out decisively.

Hence, the origin of ferromagnetism in ZnO:Li nanocrystalline powder and pellets is due to Li doping. Li incorporation in ZnO lattice in zinc substitutional site in varied amounts is confirmed from the following observed experimental facts: (i) change in lattice parameter ($a\sim0.08\%$ and $c\sim0.054\%$ for 2 at. % Li) estimated from XRD and change in Zn-O bond length from 1.9679 Å for undoped ZnO and 1.9695 Å for 2 at. % Li-doped ZnO, (ii) observation of *p*-type conductivity in ZnO which can happen only if Li goes into zinc substitutional site as shallow acceptor, and (iii) variation and increase in hole concentration with increase in Li concentration and related decrease in resistivity with increase in carrier concentration. In case of Li aggregation between ZnO nanorods, it will make Li an electron donor creating surface states. As Li itself is not a magnetic impurity, it is unlikely to have any role in magnetic ordering sitting outside the nanorods. Moreover, magnetization decreases with increase in Li concentration which should have its origin in

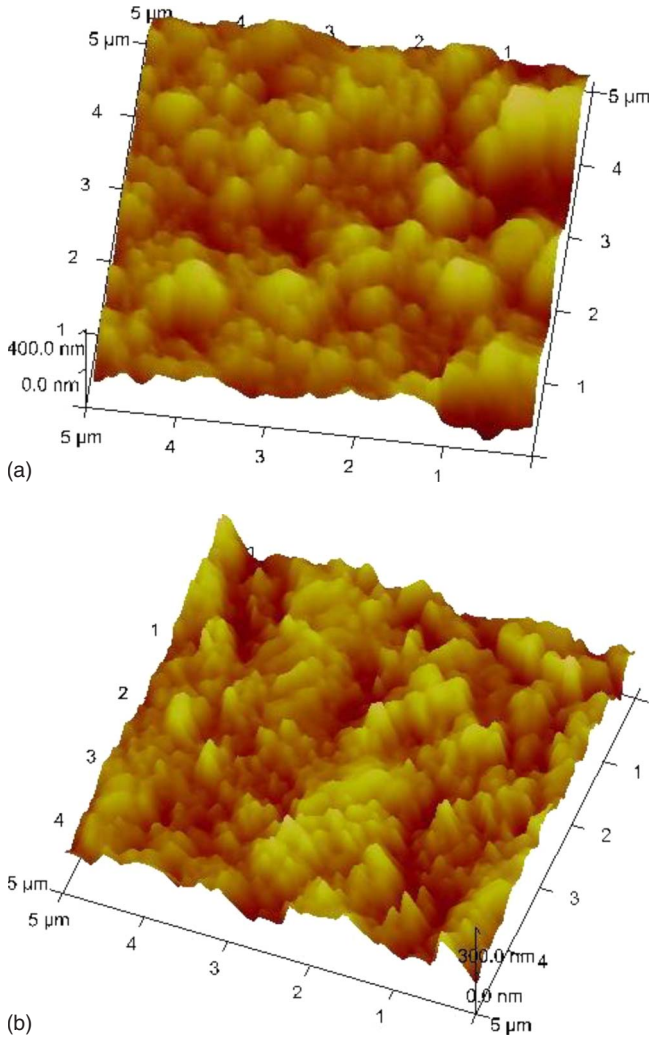

FIG. 4. (Color online) atomic force microscope (AFM) images of ZnO:Li (a) 2 at. % and (b) 10 at. % pellets.

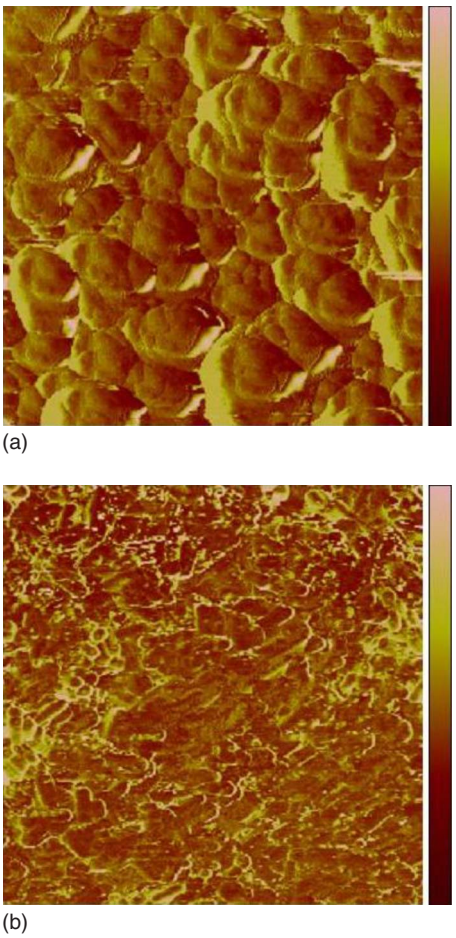

FIG. 5. (Color online) Magnetic domains visible in magnetic force microscope (MFM) image ($3\mu \times 3\mu$) of ZnO:Li (a) 2 at. % and (b) 10 at. % pellets. On the right-hand vertical color scale, pink signifies maximum magnetic force.

the strength of magnetic interaction within the lattice.

In order to strengthen experimental results of ferromagnetism in ZnO:Li, presence of magnetic domain structure was probed with the help of magnetic force microscopy. Figure 4 shows the AFM images of 2 and 10 at. % Li-doped ZnO pellets showing the variation occurring with increase in Li concentration. Figure 5 shows the MFM image of ZnO:Li (2 and 10 at. %) pellets showing formation of magnetic domains and near uniform and oriented distribution. The difference in domain morphology gives a clear indication of decrease in magnetization from 2 to 10 at. % Li doping in ZnO. As such domain formation conclusively proves the occurrence of ferromagnetism and has been reported for many DMSs,[17–19] it can be said that intrinsic ferromagnetism in ZnO is possible with the doping of spin half-alkali atom Li.

A strong and single EPR line (Fig. 6) without any hyperfine feature was observed with g value of 2.0034 and a line width of 3.5 G for as synthesized unirradiated ZnO:Li powder sample at room temperature. For detection of Li acceptor center, it has been reported that light illumination is necessary[20,21] and such spectra exhibited pronounced hyperfine structure for axial trapped hole ($g_{\parallel}=2.0028$, $g_{\perp}=2.0253$) and for nonaxial Li-O bond direction ($g_{xx}=2.0223$, $g_{yy}=2.0254$, $g_{zz}=2.0040$). Such centers have been reported to be deep acceptors producing yellow luminescence band (2.05 eV).[12] Such broad line at room temperature as observed for ZnO:Li nanocrystalline powder corresponds to FMR and is a clear indication that ferromagnetic ordering is present in ZnO:Li at room temperature. Such FMR has been reported for Mn-doped ZnO pellets[22] and quantum dots;[23] ZnO:Ni[24] and (Ga,Mn)As.[25]

PL excitation [Fig. 7(a)] and emission spectra [Fig. 7(b)] of undoped ZnO and Li-doped ZnO are similar in nature, showing same peak positions but intensity variations with change in dopant concentration. PL emission has strong near UV component peaking at 398 nm (3.11 eV), negligible visible emission, and weak near IR component at 780 nm (1.59 eV), suggesting absence of deep Li acceptor states which is reported to give PL emission at 2.05 eV.[12] PL emission peak at 398 nm corresponds to near band-edge emission of ZnO. Similar behavior has also been observed for cathodoluminescence spectra of ZnO:Li.[14] The incorporation of alkali atoms enhances the recombination process as PL intensity increases with Li doping up to 5% Li concentration and then decreases. The optical band gap measured by optical absorption

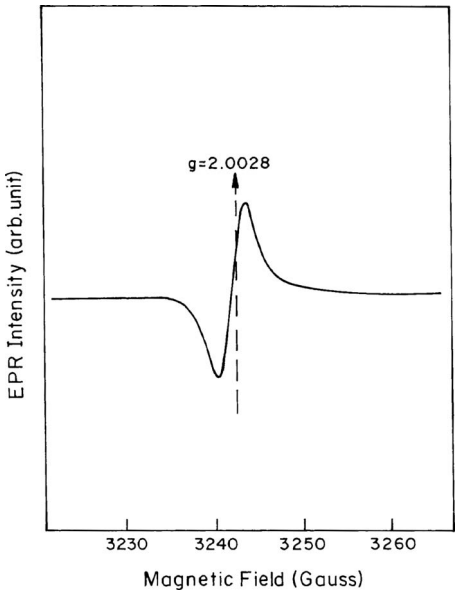

FIG. 6. EPR spectra of ZnO: Li (2 at. %) sample. The vertical line shows g value of TCNE (tetracyanoethylene) ($g=2.0028$) which was used as a standard. The broad spectra centered at $g=2.0034$ observed at room temperature correspond to ferromagnetic resonance (FMR).

is 3.19 eV for ZnO:Li. The near IR emission band (1.59 eV) is broad and Gaussian in nature, arising due to recombination between deep levels. The PL spectra of all the samples were measured under exactly identical conditions using the same sample holder, keeping every single experimental parameter such as excitation and emission slit width and filter the same. The measurements were repeated several times, and variation in intensity with Li concentration was indeed observed. Such observations indicate that Li is playing an indirect role in the PL process. Photoluminescence excitation (PLE) recorded at 398 nm emission wavelength shows a peak at 244 nm as shown in Fig. 7(a). The PLE was measured at 600 nm emission wavelength, and the plot is shown as inset in Fig. 7(a). The sharp peak at 397 nm is likely to be the excitonic absorption.

Time-resolved PL decay for ZnO:Li (2 at. %) at 398 nm emission gives exponential decay with lifetime of 1.14 ns. Such decay times have been observed for ZnO nanorods.[26] Hong *et al.*[26] showed the variation in time-resolved PL decay rate with size of ZnO nanorods for PL peak at 3.26 eV. Time constant for biexponential fit of the decay curve shows the correlation of the longer decay component with length of the nanorods. It has been shown[26] that as the length of the nanorod increases, decay rate decreases, i.e., lifetime increases. Lifetime of 190 ps and 1.4 ns was given for 600-nm-long ZnO nanorods. In our samples, length of ZnO nanorods varied from 96 to 622 nm. Hong *et al.*[26] also showed that as size of nanorods approaches the wavelength of excitation light (244 nm in our case), exciton polariton effect becomes important and the rate of radiative recombination decreases. Theoretical calculations have shown a minimum radiative lifetime of ~260 ps for nanosphere of radius 17 nm and the lifetime increases monotonically as the size increases.[27] Hence, available experimental and theoretical results indicate

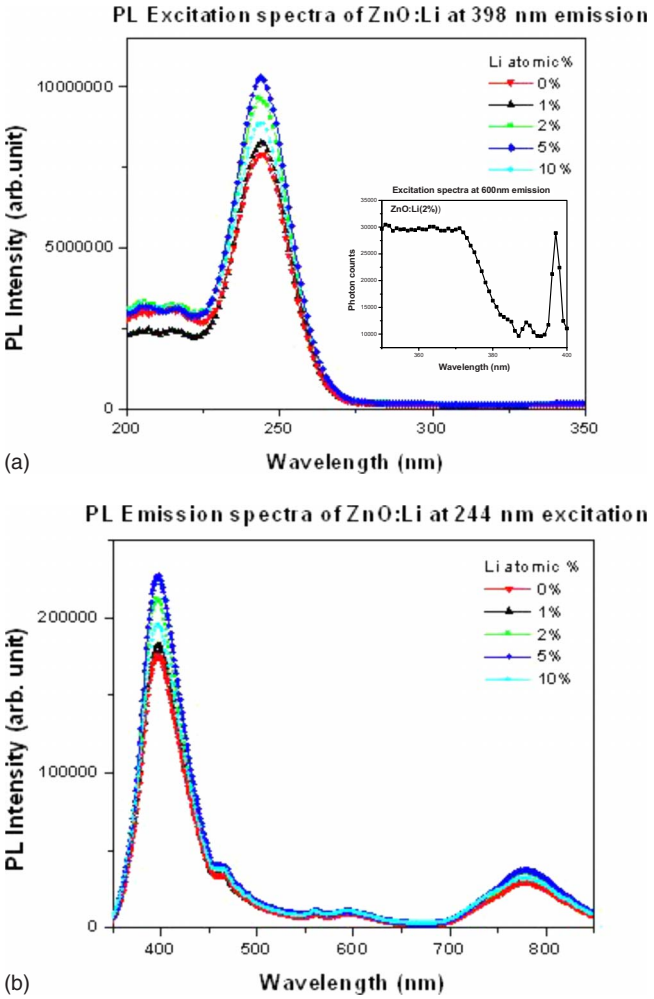

FIG. 7. (Color online) Photoluminescence (a) excitation spectra showing excitation peak at 244 nm. The inset shows the excitation spectra at 600 nm emission showing a sharp peak due to excitonic transition and (b) emission spectra showing strong peak at 398 nm.

that lifetime of 1.14 ns could arise from exciton-related decay in ZnO nanorods of present dimensions. In contrast the lifetimes for 780 nm emission are much longer and estimated to be 0.86 (77%) and 6.89 μs (23%), suggesting donor acceptor pair (DAP) recombination.

As Li is incorporated in small percentage and p-type conductivity is observed with Li doping, Li must be forming shallow acceptor levels in Zn substitutional site rather than being in interstitial position that would result in formation of donor levels. Low synthesis temperature at 500 °C which favors maximum Li incorporation,[11,14,15] p-type conductivity in ZnO:Li indicate to the fact that Li forms shallow acceptor level in substitutional Zn site. This is further strengthened by observation of strong PL peak at 3.11 eV and absence of typical PL emission arising due to deep Li acceptor levels.[12]

Ferromagnetism in ZnO lattice due to Li doping confirms the role of Li in magnetic ordering at room temperature. Based on the experimental facts in ZnO:Li material system, a physical picture of spin ordering through exchange interaction between holes trapped in oxygen $2p$ orbital adjacent to Li_{Zn}^{+} site and its propagating influence through hole media-

tion resulting in long-range ordering emerges. Induction of local magnetic moments by vacancies on neighboring atoms has been predicted from band-structure calculations.[28] Dependence on vacancy-induced local magnetic moment and magnetic coupling required for long-range ordering has been described via a single correlated band of oxygen orbitals with additional random potentials.[29] Correlated model for oxygen orbitals with random potentials representing substitutional Li atom in zinc site can be envisaged. For certain potential arising due to such defects, which in turn will depend on concentration of substitutional dopant and density of vacancies, magnetic moments would appear in oxygen sites near defects. The model proposed by Bouzerer and Ziman[29] predicts that for small potential, antiferromagnetic nearest-neighbor coupling exists. As the potential increases, the coupling becomes more ferromagnetic but with further increase some couplings become antiferromagnetic again. The model also showed that well-defined region of potential, defect concentration, as well as carrier densities exist where above room-temperature ferromagnetism and Curie temperature up to 750 K are feasible for a few percent of vacancies or substitutional impurity (Li, Na, K, etc.). Beyond the optimum window of defect concentration, T_C vanishes as magnetic couplings are destroyed by Ruderman-Kittel-Kasya-Yashida-type oscillations or antiferromagnetic superexchange. The experimental results for ZnO:Li with Li forming shallow acceptor levels fall in line with the predictions of this theory. This mechanism is very sensitive to Li concentration. Our observations show that Li incorporation that gives rise to hole concentration on the order of 10^{16} cm^{-3} is optimum for such spin ordering. More Li doping creates increased hole concentration which gradually destroys the magnetic ordering resulting in decreased magnetic moment and transition to nonferromagnetic state at a lower Curie temperature. Weak ferromagnetism arising due to vacancy or nonmagnetic dopant has been reported in oxides and other compounds;[4–8] for example, origin of ferromagnetism in oxide nanoparticles[5] has been suggested to arise from the exchange interaction between unpaired electron spins localized at oxygen vacancies lying on the nanoparticle surface. Hole dopant Li_{Zn} introduced at low synthesis temperature has been shown to promote long-range ferromagnetic coupling in ZnO:TM.[10] In the present case, dopant Li_{Zn} is able to create ferromagnetic ordering in ZnO even in the absence of any 3*d* transition metal doping. DMS has been mostly observed in thin films. Observation of ferromagnetism in an ensemble of stand alone nanoparticles, in this case in the form of nanorods, is rare. The experimental observation of occurrence of above room-temperature ferromagnetism in Li-doped ZnO explicitly reveals that it can be a promising DMS material.

IV. CONCLUSIONS

Dilute ferromagnetism at room temperature and above (up to 554 K) can be introduced in a multifunctional semiconductor such as ZnO with Li doping. Synthesis process holds the key for occurrence of *p*-type conduction and ferromagnetism in Li-doped ZnO. The intrinsic nature of ferromagnetism in ZnO:Li has been established with the experimental observation of magnetic hysteresis loop, ferromagnetic resonance and formation of magnetic domain structure. A physical model has been advanced based on substitutional Li atom creating random potential and inducing magnetic moment on oxygen atoms whose orbital is considered correlated. Such a DMS without the presence of any transition metal could be a very good option for a class of spintronic and spin light-emitting diode (LED) devices as ZnO:Li is shown to emit near UV light.

ACKNOWLEDGMENTS

We wish to thank T. K. Gundu Rao for EPR, Sukhvir Singh for TEM, Jyoti Shah for Hall effect, and Samanta for MFM measurements.

*Corresponding author; santa@nplindia.org

[1] Ü. Özgür, Ya. I. Alivov, C. Liu, A. Teke, M. A. Reschikov, S. Doğan, V. Avrutin, S. J. Cho, and H. Morkoç, J. Appl. Phys. **98**, 041301 (2005), and references therein.
[2] S. J. Pearton, C. R. Abernathy, M. E. Overberg, G. T. Thaler, D. P. Noton, N. Theodoropoulou, A. F. Hebard, Y. D. Park, F. Ren, J. Kim, and L. A. Boatner, J. Appl. Phys. **93**, 1 (2003).
[3] J. M. D. Coey, M. Venkatesan, and C. B. Fitzgerald, Nature Mater. **4**, 173 (2005).
[4] M. Venkatesan, C. B. Fitzgerald, and J. M. D. Coye, Nature (London) **430**, 630 (2004).
[5] A. Sundaresan, R. Bhargavi, N. Rangarajan, U. Siddesh, and C. N. R. Rao, Phys. Rev. B. **74**, 161306(R) (2006).
[6] D. P. Young, D. Hall, M. E. Torelli, Z. Fisk, J. L. Sarrao, J. D. Thompson, H. R. Ott, S. B. Oseroff, R. G. Goodrich, and R. Zysler, Nature (London) **397**, 412 (1999).
[7] H. Pan, J. B. Yi, L. Shen, R. Q. Wu, J. H. Yang, J. Y. Lin, Y. P. Feng, J. Ding, L. H. Van, and J. H. Yin, Phys. Rev. Lett. **99**, 127201 (2007).
[8] P. Esquinazi, D. Spemann, R. Hohne, A. Setzer, K. H. Han, and T. Butz, Phys. Rev. Lett. **91**, 227201 (2003).
[9] T. Dietl, H. Ohno, F. Matsukara, J. Cibert, and D. Ferrand, Science **287**, 1019 (2000).
[10] M. H. F. Sluiter, Y. Kawazoe, P. Sharma, A. Inoue, A. R. Raju, C. Rout, and U. V. Waghmare, Phys. Rev. Lett. **94**, 187204 (2005).
[11] Y. J. Zeng, Z. Z. Ye, W. Z. Xu, D. Y. Li, J. G. Luand, and B. H. Zhao, Appl. Phys. Lett. **88**, 062107 (2006).
[12] B. K. Meyer, N. Volbers, A. Zeuner, S. Lautenschlager, J. Sann, A. Hoffmann, and U. Haboeck, MRS Symposia Proceedings No. 891 (Materials Research Society, Pittsburgh, 2006).
[13] J. Sann, A. Hofstaetter, D. Pfisterer, J. Stehr, and B. K. Meyer, Phys. Status Solidi C **3**, 952 (2006).
[14] G. Srinivasan, R. T. Rajendra Kumar, and J. Kumar, J. Sol-Gel Sci. Technol. **43**, 171 (2007).
[15] X. H. Wang, B. Yao, Z. P. Wei, D. Z. Sheng, B. H. Li, Y. M. Lu,

D. X. Zhao, J. Y. Zhang, X. W. Fan, L. X. Guan, and C. X. Cong, J. Phys. D **39**, 4568 (2006).
[16] T. Wakano, N. Fujimura, Y. Morinaga, N. Abe, A. Asgida, and T. Ito, Physica E (Amsterdam) **10**, 260 (2001).
[17] J. Philip, A. Punnoose, B. I. Kim, K. M. Reddy, S. Layne, J. O. Holmes, B. Satpati, P. R. Leclair, T. S. Santos, and J. S. Moodera, Nature Mater. **5**, 298 (2006).
[18] H. C. Jeon, Y. S. Jeong, T. W. Kang, T. W. Kim, K. J. Chung, K. J. Chung, W. Jhe, and S. A. Song, Adv. Mater. (Weinheim, Ger.) **14**, 1725 (2002).
[19] M. Diaconu, H. Schimdt, H. Hochmuth, M. Lorentz, G. Benndorf, J. Lenzner, D. Spemann, A. Setzer, K. Nielsen, P. Esquinazi, and M. Grundmann, Thin Solid Films **486**, 117 (2005).
[20] O. F. Schirmer, J. Phys. Chem. Solids **29**, 1407 (1968).
[21] S. M. Evans, N. C. Giles, L. E. Haliburton, and L. A. Kappers, J. Appl. Phys. **103**, 043710 (2008).
[22] P. Sharma, A. Gupta, K. V. Rao, F. J. Owens, R. Sharma, R. Ahuja, and J. M. Osorio-Guillen, b. Johansson, and G. A. Gehring, Nature (London) **2**, 673 (2003).
[23] N. S. Norberg, K. R. Kittilstvlrd, J. E. Amonette, R. K. Kukkadapu, D. A. Schwartz, and D. R. Gamelin, J. Am. Chem. Soc. **126**, 9387 (2004).
[24] V. Castel, J. B. Youssef, and C. Brosseau, J. Nanomater., Special Issue 1, **2007** (2007)
[25] M. Rubinstein, A. Hanbicki, P. Lubitz, J. J. Krebs, and B. Jonker, J. Magn. Magn. Mater. **250**, 164 (2002).
[26] S. Hong, T. Joo, W. Park, Y. H. Jun, and G. Yi, Appl. Phys. Lett. **83**, 4157 (2003).
[27] B. Gil and A. V. Kavokin, Appl. Phys. Lett. **81**, 748 (2002).
[28] J. Osorio-Guillen, S. Lany, S. V. Barabash, and A. Zunger, Phys. Rev. Lett. **96**, 107203 (2006).
[29] G. Bouzerar and T. Ziman, Phys. Rev. Lett. **96**, 207602 (2006).